

X-ray diffraction study of amorphous Fe-Ti alloys

This article has been downloaded from IOPscience. Please scroll down to see the full text article.

1990 J. Phys.: Condens. Matter 2 9967

(<http://iopscience.iop.org/0953-8984/2/50/001>)

View [the table of contents for this issue](#), or go to the [journal homepage](#) for more

Download details:

IP Address: 171.66.16.96

The article was downloaded on 10/05/2010 at 22:45

Please note that [terms and conditions apply](#).

X-ray diffraction study of amorphous Fe–Ti alloys

Hideyuki Yasuda, Kenji Sumiyama† and Yoji Nakamura‡

Department of Metal Science and Technology, Kyoto University, Kyoto 606, Japan

Received 21 June 1990

Abstract. X-ray diffraction measurements were carried out for amorphous alloys $\text{Fe}_{1-x}\text{Ti}_x$ with x from 0.2 to 0.75. The radial distribution function, $g(r)$, shows a clear first peak and a shoulder beyond the second peak. The $g(r)$ is insensitive to the alloy concentration, which is explained by a simple model based on the spiral tetrahedral stacking. No chemical short-range order has been detected.

1. Introduction

Systematic studies of sputter-deposited Fe-based binary alloys produced by sputter deposition (Sumiyama and Nakamura 1983, Fukamichi and Gambino 1983) indicate that Fe forms an amorphous phase with early 3d transition metals such as Sc, Ti and V. Sputter-deposited $\text{Fe}_{1-x}\text{Ti}_x$ alloys are a typical example of metal–metal amorphous alloys: the amorphous phase is obtained for $0.2 < x < 0.75$, where the Ti concentration range covers the Laves phase (C14), TiFe_2 , the ordered phase (B2), FeTi, and the metastable intermetallic compound (E9_3), Ti_2Fe . Amorphous $\text{Fe}_{1-x}\text{Ti}_x$ alloys show high thermal stability: the highest crystallization temperature of 950 K is obtained at $x = 0.3\text{--}0.4$ where the Laves phase is formed in the equilibrium phase diagram (Sumiyama *et al* 1987). The amorphous $\text{Fe}_{1-x}\text{Ti}_x$ alloys are ferromagnets at low temperatures (Sumiyama and Nakamura 1983, Liou and Chien 1984) and reveal an Invar-type thermal expansion anomaly (Fukamichi *et al* 1982). These alloys display no cluster-glass behaviour but show characteristics of a weak itinerant electron ferromagnet (Sumiyama *et al* 1990).

It has been reported that the forming ability of an amorphous phase is enhanced by alloying, because the addition of atoms with a different size leads to distortions of radial and angular configurations of the atomic stacking topological effect and the chemical effect of a preferential bonding between different atoms (Suzuki *et al* 1976). The alloying also affects the thermal stability and physical properties of amorphous alloys. An amorphous phase has been obtained only in a narrow concentration range when the chemical short-range order is predominant, while it is widely obtained when the topological disorder is predominant. In these respects, it is interesting to study the structure of amorphous $\text{Fe}_{1-x}\text{Ti}_x$ alloys as a function of alloy concentration. In this paper we present x-ray diffraction experiments on bulk amorphous $\text{Fe}_{1-x}\text{Ti}_x$ alloys.

† Present address: Institute of Materials Research, Tohoku University, Sendai 980, Japan.

‡ Present address: Faculty of Science and Technology, Ryukoku University, Ohtsu 520, Japan.

2. Experimental procedure

Bulk Fe–Ti alloy specimens from 50 to 100 μm in thickness were prepared by facing-targets-type DC sputtering on glass or silicon wafer substrates. We kept the substrate at about 350 K by indirect water cooling during the sputter deposition. The alloy concentration was adjusted by changing the ratio of the surface areas of Fe (99.9%) and Ti (99.9%) plates of composite targets. The chemical composition of deposited alloys was determined by electron probe microanalysis (EPMA).

X-ray diffraction measurements were made at 290 K using Mo $K\alpha$ radiation. A graphite monochromator was used to eliminate the fluorescent x-rays and $K\beta$ radiation from specimens. The x-ray intensity was measured stepwise as a function of the scattering angle in two 2θ ranges, one from 10° to 30° and the other from 20° to 100° . The intensity of the low-angle part was smoothly connected to that of the high-angle part and the structure factor, $a(S)$, was obtained by normalization. Here S is the scattering vector.

The radial distribution function, $G(r)$, was calculated from $a(S)$ by equation (1), and the reduced distribution function, $g(r)$, from equation (2):

$$G(r) = 4\pi r^2 \sum_{i,j} c_i K_i K_j g_{ij}(r) \\ = 4\pi r^2 \left(\sum_i c_i K_i \right)^2 \rho + \frac{2r}{\pi} \left(\sum_i c_i K_i^2 \right) \int_0^\infty S(a(S) - 1) \sin Sr \, dS \quad (1)$$

$$g(r) = G(r) \left[4\pi r^2 \left(\sum_i c_i K_i \right)^2 \rho \right]^{-1} \quad (2)$$

Here c_i and K_i are the atomic concentration and the average electron number of the i th element, respectively. The atomic density, ρ , was estimated from the theoretical dependence of $G(r) = 0$ for small r .

3. Results

Figures 1(a) and (b) show the structure factor, $a(S)$, of amorphous $\text{Fe}_{1-x}\text{Ti}_x$ alloys. No significant concentration dependence was observed for these alloys, although the peak positions of $a(S)$ shift, mainly due to the difference in the atomic radii of Fe and Ti. We observed the sharp first peak and an overlap of the second and third peaks in $a(S)$, where the third peak appears as a shoulder of the second peak. Such a characteristic pattern in $a(S)$ has also been observed in many amorphous metals and alloys. The oscillation of $a(S)$ was observed up to about 10 \AA^{-1} and then decays rapidly for alloys richer in Ti.

Figures 2(a) and 2(b) show the reduced radial distribution function, $g(r)$. The sharp first peak of $g(r)$ is composed of nearest-neighbour atom pairs of Fe–Fe, Fe–Ti and Ti–Ti. The first-neighbour distance indicated by the position of the first peak is slightly shorter than that expected from the Goldschmidt radii of Fe and Ti atoms, probably because of the charge transfer between Fe and Ti atoms (Liou and Chien 1984, Sumiyama *et al* 1986). The third peak is observed as a shoulder of the second peak in $g(r)$. The atomic correlations in $g(r)$ are detected in the range of r up to 10 \AA . As listed in table 1, the peak positions of $g(r)$ shift with the change of concentration ratio of Fe and Ti atoms. When the peak position is scaled to the first peak position of $g(r)$, the relative peak position is almost independent of

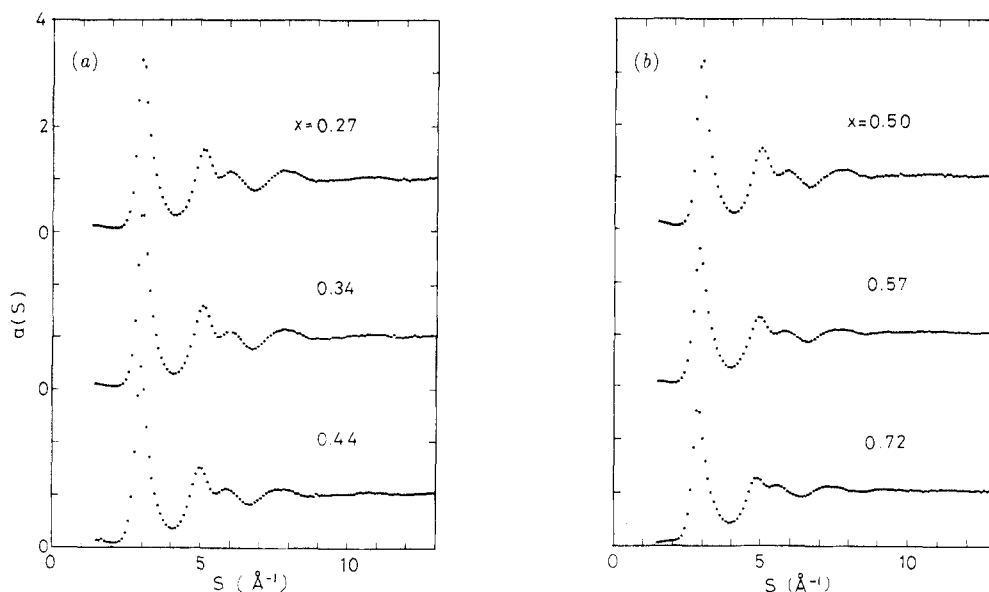


Figure 1. Structure factors, $a(S)$, of amorphous $\text{Fe}_{1-x}\text{Ti}_x$ alloys. (a) $x < 0.50$; (b) $x \geq 0.50$.

Table 1. Peak positions of $g(r)$ for amorphous $\text{Fe}_{1-x}\text{Ti}_x$ alloys. The numbers under each peak position indicate the relative peak position scaled to the first peak.

x	$g(r)$ (\AA)			
	r_1	r_2	r_3	r_4
0.27	2.56	4.25	5.05	6.50
	1	1.66	1.97	2.53
0.34	2.57	4.25	5.11	6.48
	1	1.65	1.99	2.57
0.44	2.60	4.30	5.15	6.60
	1	1.65	1.98	2.54
0.50	2.64	4.36	5.23	6.68
	1	1.65	1.98	2.53
0.57	2.70	4.43	5.28	6.80
	1	1.64	1.96	2.54
0.72	2.78	4.60	5.40	6.95
	1	1.65	1.94	2.50

alloy concentration as listed in table 1. Ignoring the effect of chemical short-range order, this behaviour suggests no marked structural change in the concentration range between $x = 0.2$ and $x = 0.75$.

As shown in figure 3, the average coordination number as estimated from the integrated intensity of the first peak in $g(r)$ is about 11.5 and is independent of alloy concentration within the experimental error.

Figure 4 shows the concentration dependence of the atomic density, ρ , estimated from the radial distribution function, $G(r)$. In amorphous $\text{Fe}_{1-x}\text{Ti}_x$ alloys ρ decreases monotonically with increasing x . The values of ρ for the amorphous alloys are 9.5% smaller than those of the

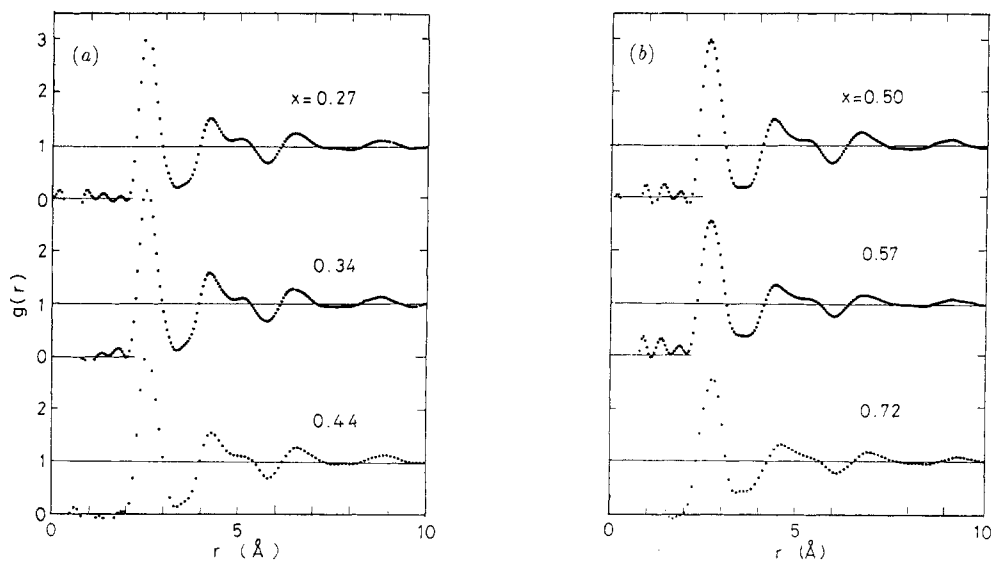


Figure 2. Reduced radial distribution functions $g(r)$ of amorphous $\text{Fe}_{1-x}\text{Ti}_x$ alloys. (a) $x < 0.50$; (b) $x \geq 0.50$.

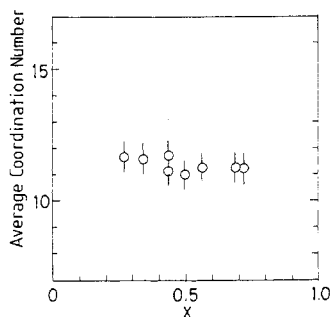


Figure 3. Average coordination number of amorphous $\text{Fe}_{1-x}\text{Ti}_x$ alloys.

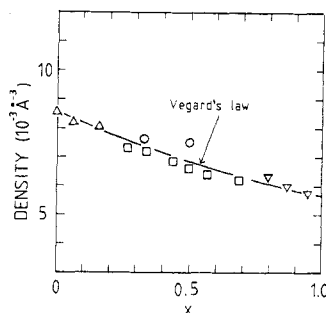


Figure 4. Atomic densities, ρ , of amorphous $\text{Fe}_{1-x}\text{Ti}_x$ alloys (\square), α -Fe-type solid solutions (Δ), β -Ti-type solid solutions (∇) and intermetallic compounds (\circ). The full curve is estimated from Végard's law.

ordered FeTi compound and only 5% smaller than that estimated from Végard's law, indicating that the amorphous alloys have a dense atomic packing.

4. Discussion

As shown in figures 1 and 2, the $a(S)$ and $g(r)$ of amorphous $\text{Fe}_{1-x}\text{Ti}_x$ alloys show no marked concentration dependence except for a rapid decay of the $a(S)$ oscillation and a rapid broadening of $g(r)$ peaks in Ti-rich alloys. This means that the richer the alloy is in Ti, the weaker its average interatomic potential. Systematic studies of x-ray diffraction of liquid 3d transition metals indicate that the oscillations of $a(S)$ in early transition metals such as V and Ti are smaller than those of late transition metals, Cr, Fe, Co, Ni and Cu (Waseda and Tamaki

1975). It has been reported that d electrons play an important role in the cohesion of transition metals (Friedel and Sayer 1977) and the oscillation decay is ascribed to the d electrons. Metallic amorphous alloys containing transition elements are classified into four groups: (i) pure metals, (ii) transition metal–transition metal alloys, (iii) rare earth–transition metal alloys and (iv) metal–metalloid alloys. In amorphous alloys of group (iii), the difference in the atomic size of constituent elements is very large and few peaks, corresponding to nearest-neighbour atoms, were observed in $g(r)$ (Matsuura *et al* 1988). The amorphous $\text{Fe}_{1-x}\text{Ti}_x$ alloys belong to group (ii) and the atomic size difference is relatively small: the atomic size ratio, $r_{\text{Ti}}/r_{\text{Fe}}$, is 1.17 and no clear chemical correlation is observed in $g(r)$. Few studies have been reported for the structure of amorphous alloys of group (1), and electron diffraction patterns have been observed for amorphous Fe and Ni films (Ichikawa 1973). The amorphous Fe film also shows that the third peak appears as a shoulder of the second peak in the diffraction pattern. This behaviour is similar to the corresponding feature of $a(S)$ of amorphous $\text{Fe}_{1-x}\text{Ti}_x$ alloys and the relative peak positions are also consistent with the present results, suggesting a structural similarity between the amorphous Fe film and the amorphous $\text{Fe}_{1-x}\text{Ti}_x$ alloys.

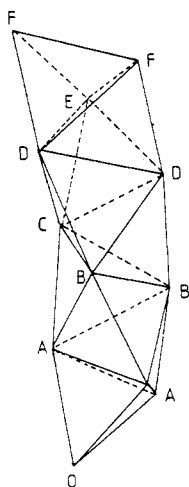
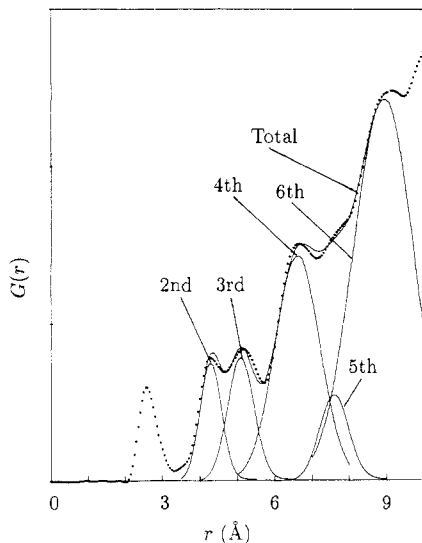


Figure 5. Spiral polytetrahedral cluster model (after Takeuchi and Kobayashi 1981). Average radial distances are $OA = 1$, $OB = 1.65$, $OC = 1.99$, $OD = 2.49$, $OE = 2.97$ and $OF = 3.38$, respectively.

The radial distribution function of amorphous metals has been interpreted by a spiral polytetrahedral cluster model shown in figure 5 (after Takeuchi and Kobayashi 1981): the amorphous structure is constructed as a sequential stack of tetrahedra. Within this model the relative peak positions scaled by the first peak are 1, 1.65, 1.99, 2.49 respectively. These peak positions well agree with the estimated results of the present amorphous $\text{Fe}_{1-x}\text{Ti}_x$ alloys, as listed in table 1. In order to discuss the validity of this model, we decompose the $G(r)$ curve of amorphous $\text{Fe}_{0.73}\text{Ti}_{0.27}$ alloys into the individual atomic shells expected from this model. Assuming the distribution curve of each atomic shell to be Gaussian, the $G(r)$ curve is well reproduced by the contributions of these atom pairs, as shown in figure 6. Table 2 shows the experimental coordination numbers of several atomic shells and those calculated from a geometrical consideration of the above model. The coordination numbers of the second and third peaks as derived from theory and experiment are quite different, while the sums of the

Table 2. Coordination numbers of several atomic shells expected from a spiral polytetrahedral cluster model for the amorphous alloy $\text{Fe}_{0.73}\text{Ti}_{0.27}$.

	$g(r)$						Total
	1st	2nd	3rd	4th	5th	6th	
Experiment	11.7	17	22	69	17	158	295
Model	13.4	30.8	13.4	91.7	13.4	182	345

**Figure 6.** Radial distribution function, $G(r)$, of the amorphous alloys $\text{Fe}_{0.73}\text{Ti}_{0.27}$. The dotted curve indicates the experimental result. The full curves indicate individual atomic shells expected from a spiral polytetrahedral cluster model.

numbers of these two peaks are nearly the same. This difference could be attributed to the geometrical considerations in this model being too simple.

Although the spiral polytetrahedral cluster model assumes a simple stacking of a same kind of atoms, a better fit is obtained by making the widths of model distribution peaks wider, indicating that the actual amorphous $\text{Fe}_{1-x}\text{Ti}_x$ alloys are composed of distorted tetrahedra. In the dense random packing of hard spheres (DRPHS) model for an amorphous structure (Finney 1970), the dominant coordination polyhedron is an icosahedron, which is composed of tetrahedra. Figure 7 shows the number of atomic bonds as a function of the number of atoms in a sequentially stacked cluster. The number of bonds of the icosahedral cluster is larger than that of the BCC or FCC structure, suggesting that the icosahedral cluster is the most stable among small clusters as long as the number of nearest interatomic bonds is predominant. Since the icosahedral unit cannot densely fill a large space and satisfy a translational symmetry, a wide variety of numbers, spacings and angular distributions are introduced in constructing a dense solid. Therefore, the spiral polytetrahedral cluster model is consistent with the DRPHS model and the repulsive parts of interatomic or hard core potentials of constituent atoms play a dominant role in determining the structure of amorphous $\text{Fe}_{1-x}\text{Ti}_x$ alloys. This atomic distribution has been estimated from the analysis of the quadrupole splitting in the Mössbauer spectra for

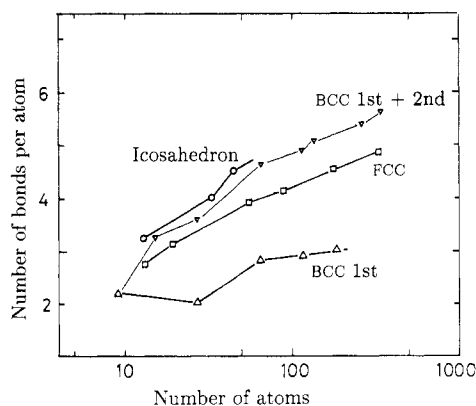


Figure 7. Correlation between the number of nearest interatomic bonds and the number of atoms in a cluster. For a BCC structure two cases are plotted: one includes only the first neighbour, and the other both the first and second neighbours.

amorphous Fe–Ti alloys (Sumiyama *et al* 1986).

The chemical short-range order is not taken into account in the present analysis. Neutron diffraction measurements also suggest little or no chemical short-range order in amorphous Fe–Ti alloys (Rodmacq *et al* 1987). Moreover, our recent EXAFS experiments indicate no chemical short-range order in these alloys (Yasuda *et al* 1990). However, the high thermal stability of amorphous $\text{Fe}_{1-x}\text{Ti}_x$ alloys suggests that an alloying of Fe and Ti atoms affects the thermal stability of the amorphous structure: local strain induced by the difference of size of Fe and Ti atoms is relaxed and the stacking of distorted tetrahedra is stabilized in the amorphous structure. Therefore, the amorphous $\text{Fe}_{1-x}\text{Ti}_x$ alloys obtained by sputter deposition are topologically random and homogeneous.

Acknowledgments

The authors wish to thank Dr H Ohno of the Japan Atomic Energy Research Institute for his support in performing the x-ray diffraction analysis. They also thank Mr R Iehara for his technical support, Mr T Unesaki for EPMA measurements and Mr S Kambara, Nihon Kogyo Co. Ltd. for supplying Ti targets. This work was partially supported by a Grant-in-Aid for Developmental Scientific Research given by the Ministry of Education, Science and Culture, Japan.

References

- Finney J L 1970 *Proc. R. Soc. A* **319** 479–93
- Friedel J and Sayer C M 1977 *J. Physique* **38** 697–705
- Fukamichi K and Gambino R J 1983 *IEEE Trans. Magn.* **MAG-35** 3059–61
- Fukamichi K, Hiroyoshi H, Kaneko T and Masumoto T 1982 *J. Appl. Phys.* **53** 8107–9
- Ichikawa T 1973 *Phys. Status Solidi a* **19** 707–16
- Liou S H and Chien C L 1984 *J. Appl. Phys.* **55** 1820–2
- Matsuura M, Fukamichi K, Fukunaga K, Sato Y and Suzuki K 1988 *Z. Phys. Chem., NF* **157** 85–9
- Rodmacq B, Maret M, Lancon F and Chamberod A 1988 *Mater. Sci. Eng.* **97** 157–61

- Sumiyama K, Ezawa H and Nakamura Y 1986 *Phys. Status Solidi a* **93** 81–6
— 1987 *Acta Metall.* **35** 1221–8
Sumiyama K and Nakamura Y 1983 *J. Magn. Magn. Mater.* **25** 219–20
Sumiyama K, Yasuda H and Nakamura Y 1990 *J. Phys.: Condens. Matter* **2** 3595–610
Suzuki K, Fukunaga T, Misawa M and Masumoto T 1976 *Mater. Sci. Eng.* **23** 215–8
Takeuchi S and Kobayashi S 1981 *Phys. Status Solidi a* **65** 315–20
Waseda Y and Tamaki S 1975 *Phil. Mag.* **32** 273–81
Yasuda H, Sumiyama K and Nakamura Y 1988 *Trans. Japan Inst. Met. Suppl.* **29** 139–42
— 1990 in preparation